

Supporting Information

for

Preparation of nickel-bound porous carbon and its application in supercapacitors

Liangyu Liu^{a,b}, Yixin Li^a, Yanan Meng^a, Ying Xue^a, Bin Yang^{b*}, Bing Li^{b*} and Xiaoyang Liu^{a*}

a. State Key Laboratory of Inorganic Synthesis and Preparative Chemistry, College of Chemistry, Jilin University, Changchun 130012, China. Tel/Fax: +86-431-85168316. E-mail: liuxy@jlu.edu.cn

b. Center for High Pressure Science and Technology Advanced Research, Changchun 130012, China.

* Corresponding authors: Xiaoyang Liu (liuxy@jlu.edu.cn); Bing Li (libing@hpstar.ac.cn); Bin Yang (yangbin@hpstar.ac.cn)

1. Preparation process of the working electrode

The working electrode was obtained by pressing the active material film on the nickel foam (~1 cm²). The film was created as a result of mixing active material (80 wt%), acetylene black (15 wt%), polytetrafluoroethylene (5 wt%), and a small amount of ethanol followed by grounding and flattening. After the process, the electrode was dried in an oven at 60°C for 2 h before testing

Figure S1

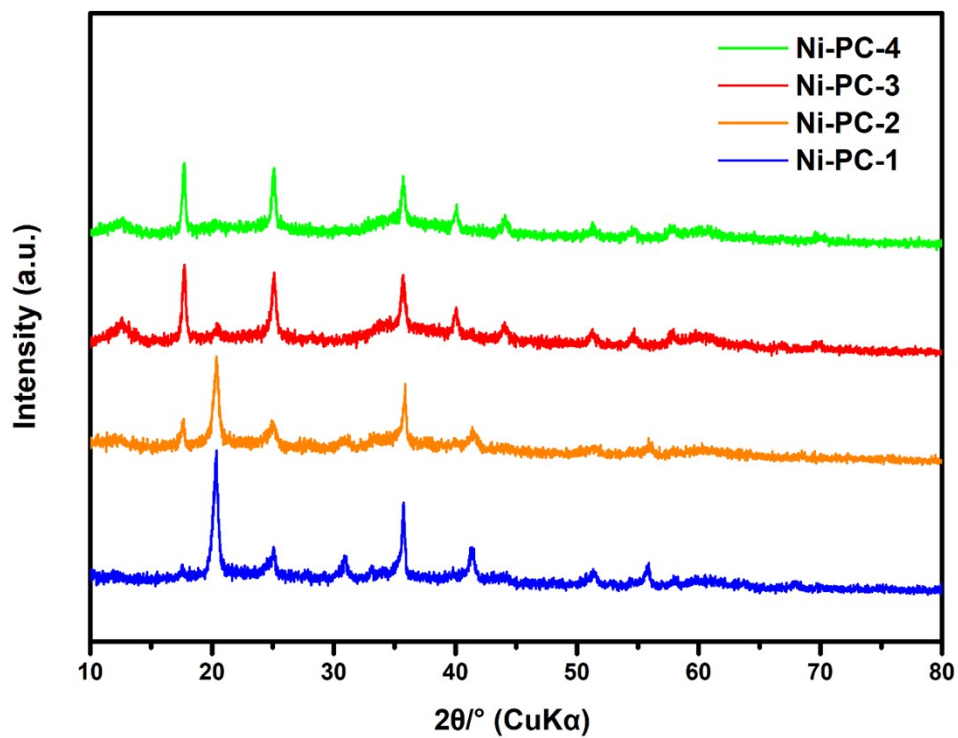


Figure S1. XRD patterns of Ni-PC-1, Ni-PC-2, Ni-PC-3 and Ni-PC-4.

Figure S2

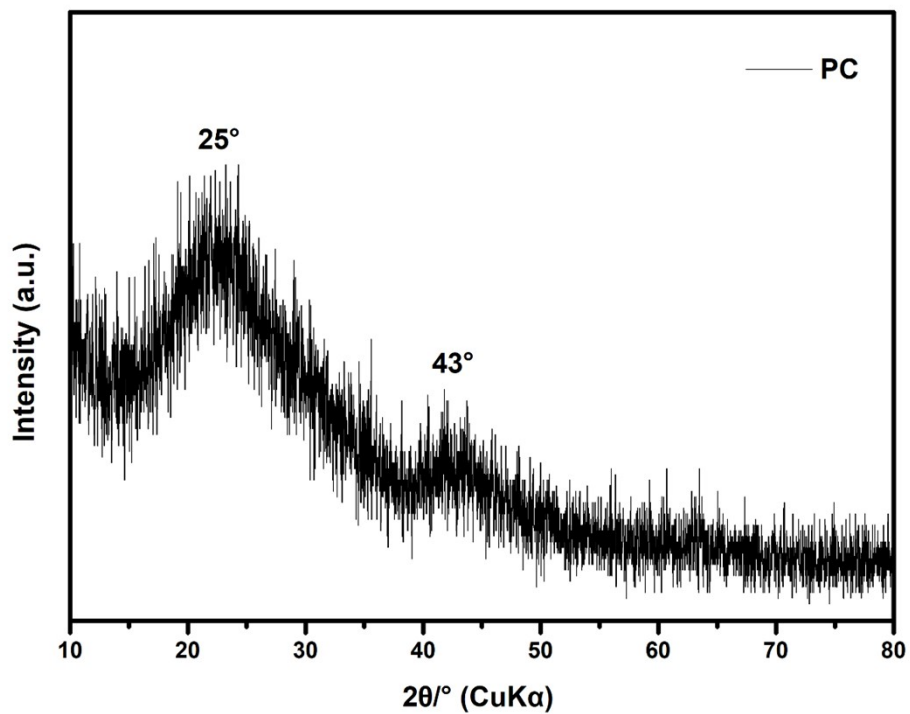


Figure S2. XRD pattern of PC.

Figure S3

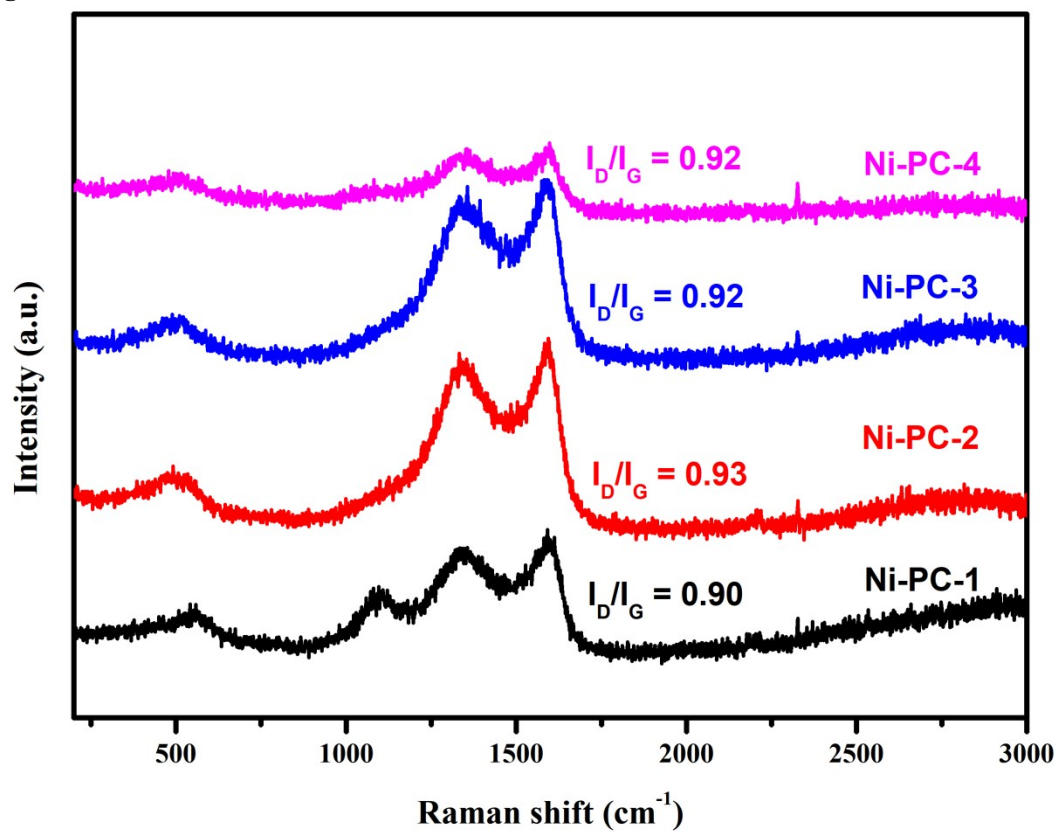


Figure S3. Raman spectra of Ni-PC-1, Ni-PC-2, Ni-PC-3 and Ni-PC-4.

Figure S4

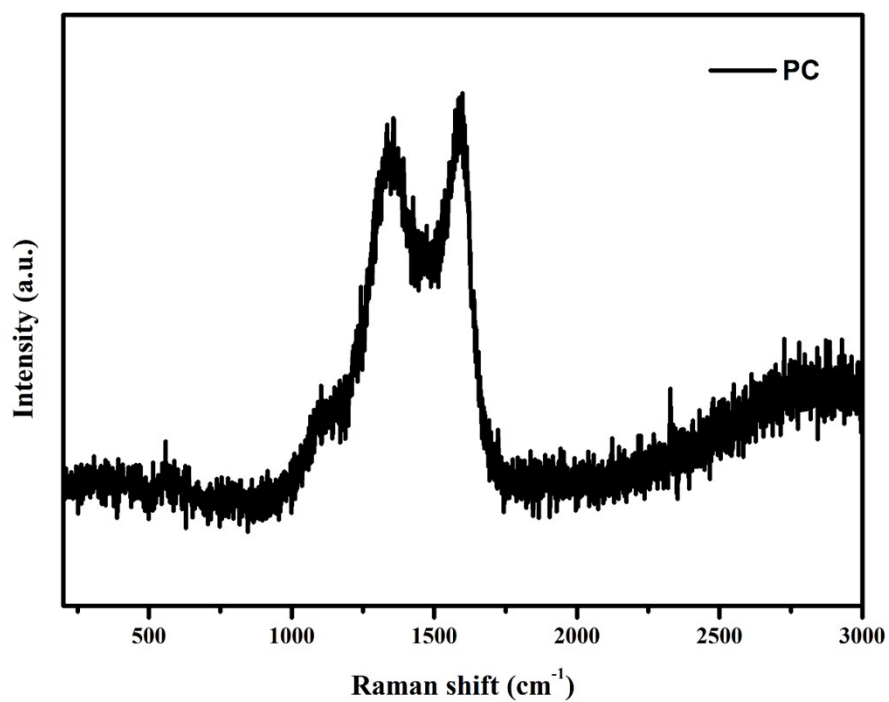


Figure S4. Raman spectrum of PC.

Figure S5

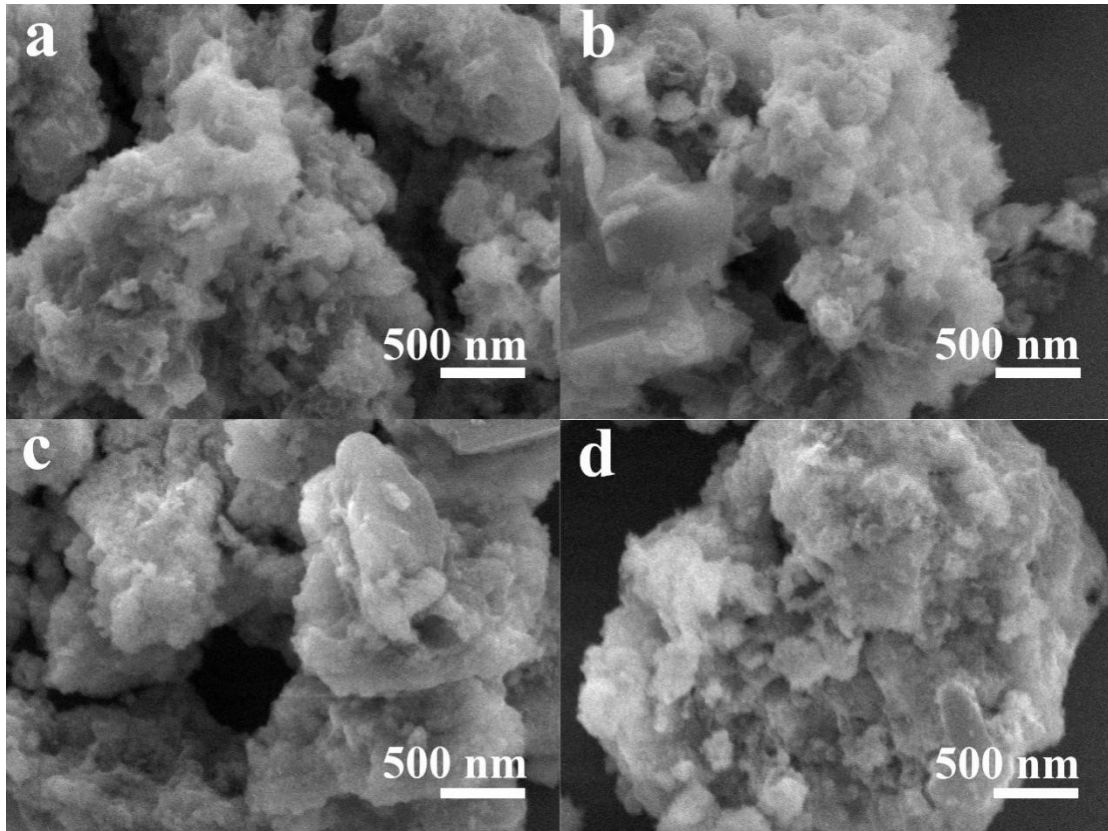


Figure S5. SEM images of Ni-PC-1 (a), Ni-PC-2 (b), Ni-PC-3 (c) and Ni-PC-4 (d).

Figure S6

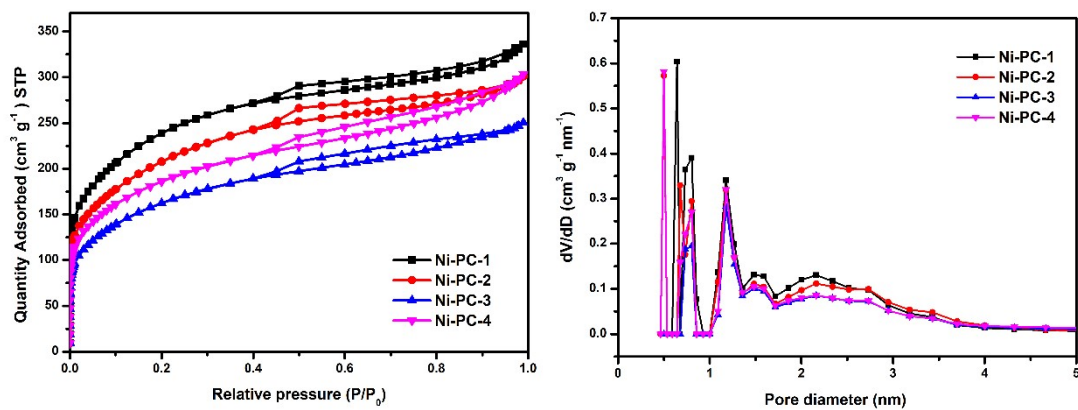


Figure S6. The nitrogen adsorption-desorption curves (a) and the pore size distribution curves (b) of Ni-PC-1, Ni-PC-2, Ni-PC-3 and Ni-PC-4.

Figure S7

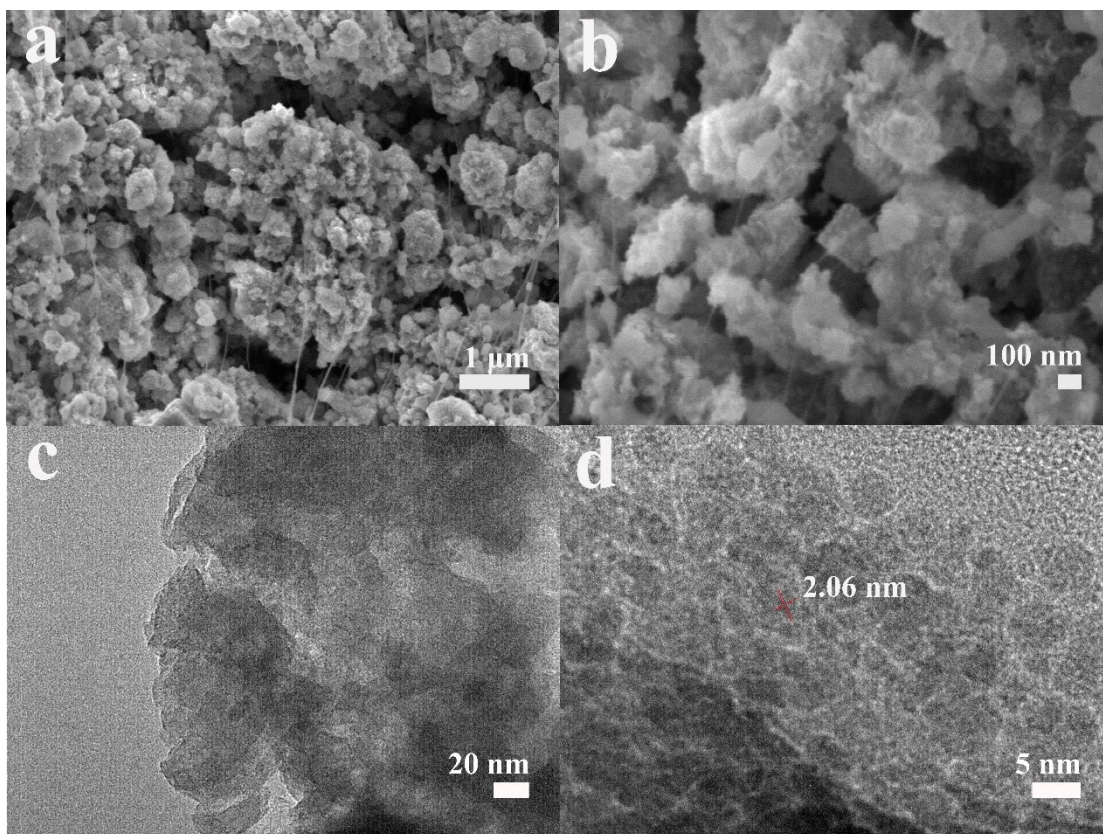


Figure S7. SEM (a, d), TEM (c), and HRTEM (d) images of Ni-PC-2 after the after the electrochemical experiment.

Figure S8

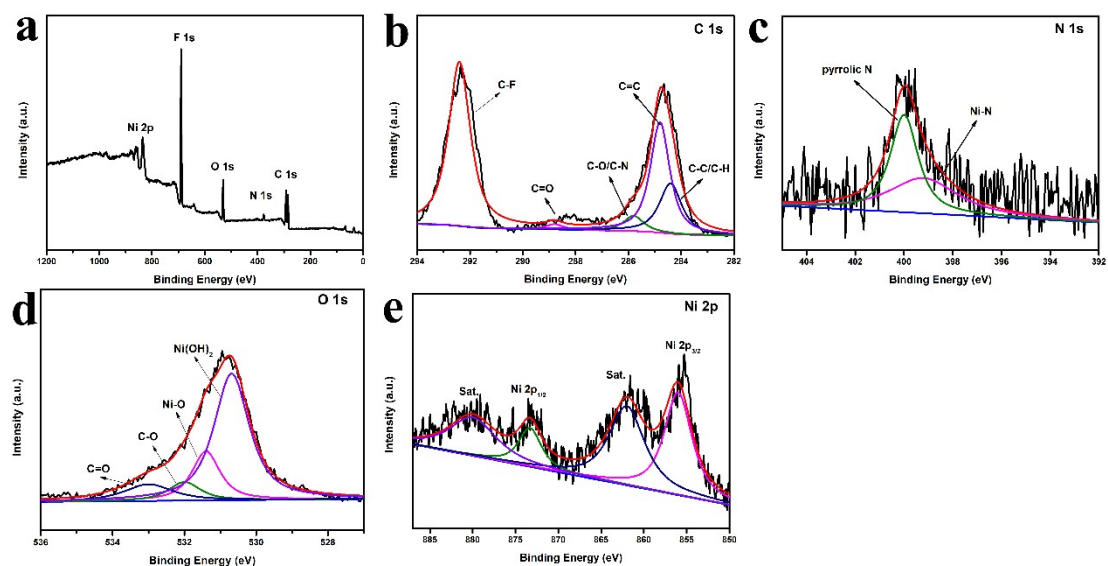


Figure S8. XPS spectra of Ni-PC-2 after the electrochemical experiment: (a) Survey XPS; (b–e) High-resolution XPS spectra of C_{1s} , N_{1s} , O_{1s} , and Ni_{2p} , respectively.

Figure S9

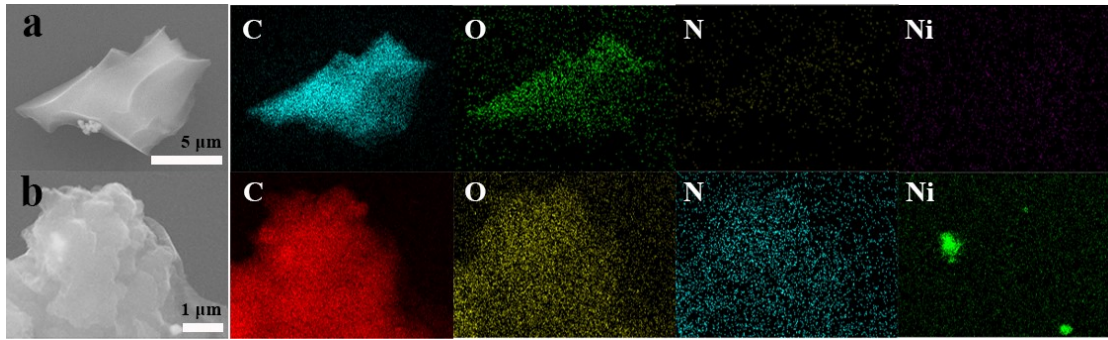


Figure S9. The SEM image and corresponding elemental mapping images of C, O, N, and Ni for Ni-PC-s-4 (a) and Ni-PC-p-16 (b).

Figure S10

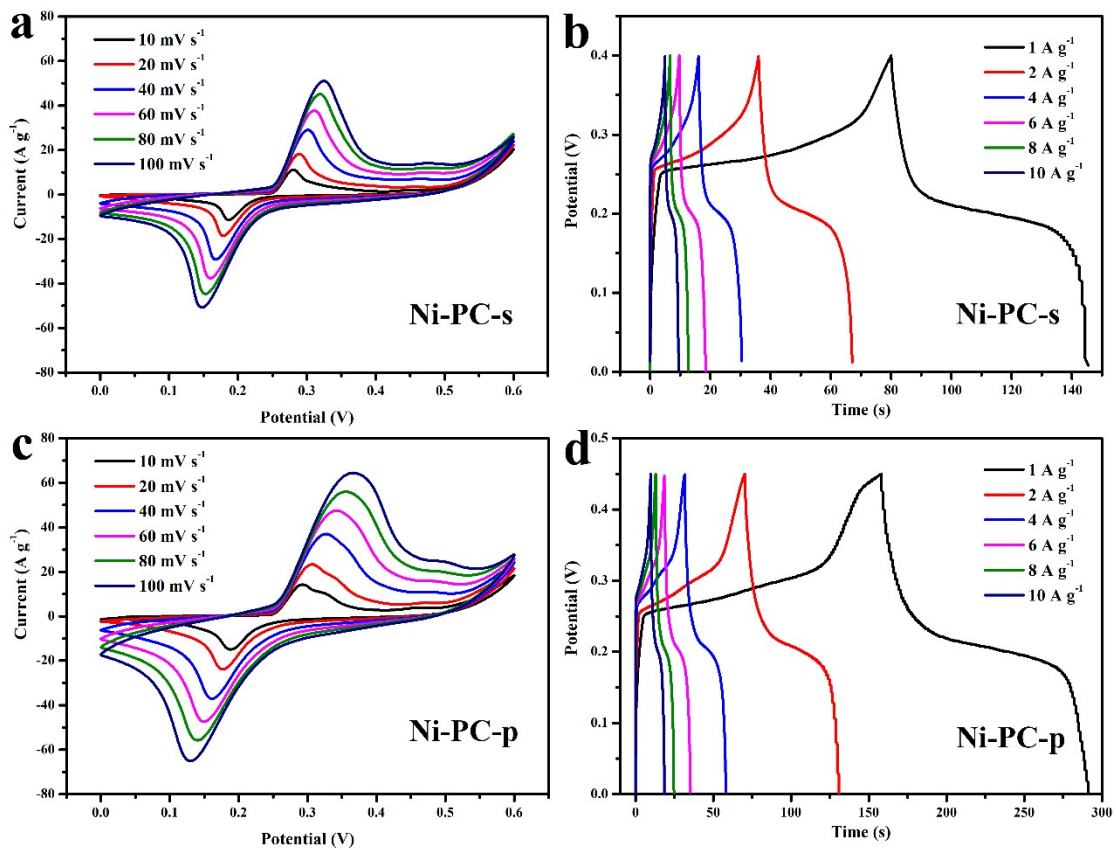


Figure S10. (a) CV and (b) GCD curves of Ni-PC-s; (c) CV and (d) GCD curves of Ni-PC-p.

Table S1. The specific capacitance and cyclic stability of Ni-PC-1, Ni-PC-2, Ni-PC-3,

and Ni-PC-4.

	Capacitance (F g ⁻¹)	Cycling capability (after 10000 cycles)
Ni-PC-1	522.5	111.5%
Ni-PC-2	565	105.8%
Ni-PC-3	427.5	69.3%
Ni-PC-4	285.0	95.4%
Ni-PC-s-x	163.5	98.8%
Ni-PC-p-4	178.9	83.3%
Ni-PC-p-8	198.4	106.7%
Ni-PC-p-16	295.6	120.7%
Ni-PC-p-32	282.4	150.4%
